Final Report

June 1975

EXAMINATION OF STEEL SPECIMENS IMPACTED AT HYPERVELOCITY

By: D. A. HOCKEY and D. R. CURRAN

Prepared for:

MOBILITY EQUIPMENT RESEARCH AND DEVELOPMENT CENTER
FORT BELVOIR, VIRGINIA 22060
Attention: DR. J. W. BOND, JR.

CONTRACT DAAK02-75-C-0044

STANFORD RESEARCH INSTITUTE
Menlo Park, California 94025 · U.S.A.

UNCLASSIFIED

SECURITY CLASSIFICATION OF THIS PAGE (When Data Entered)

REPORT DOCUMENTATION PAGE

READ INSTRUCTIONS BEFORE COMPLETING FORM

1. REPORT NUMBER

2. GOVT ACCESSION NO.

3. RECIPIENT'S CATALOG NUMBER

4. TITLE (and Subtitle)

(6) EXAMINATION OF STEEL SPECIMENS IMPACTED AT HYPERVELOCITY.

5. TYPE OF REPORT & PERIOD COVERED

(9) Final Report,
23 Sep [redacted]74
22 Jun [redacted]75,

6. PERFORMING ORG. REPORT NUMBER

(16) SRI - PYU-3754

7. AUTHOR(s)

(10) D. A. Shockey D. R. Curran

8. CONTRACT OR GRANT NUMBER(s)

(15) DAAK02-75-C-0044

9. PERFORMING ORGANIZATION NAME AND ADDRESS

Stanford Research Institute
333 Ravenswood Avenue
Menlo Park, CA 94025

10. PROGRAM ELEMENT, PROJECT, TASK AREA & WORK UNIT NUMBERS

(12) 35 p.

11. CONTROLLING OFFICE NAME AND ADDRESS

12. REPORT DATE

(11) Jun [redacted]75

13. NO. OF PAGES

42

14. MONITORING AGENCY NAME & ADDRESS (if diff. from Controlling Office)

Mobility Equipment Research & Development Center
Fort Belvoir, Virginia 22060

15. SECURITY CLASS. (of this report)

UNCLASSIFIED

15a. DECLASSIFICATION/DOWNGRADING SCHEDULE

16. DISTRIBUTION STATEMENT (of this report)

DIST[illegible] STATEMENT A
Approved for public release;
Distribution Unlimited

DDC
RECEIVED
JAN 8 1976

17. DISTRIBUTION STATEMENT (of the abstract entered in Block 20, if different from report)

A

18. SUPPLEMENTARY NOTES

19. KEY WORDS (Continue on reverse side if necessary and identify by block number)

Hypervelocity impact
Steel target plates
Backface fragmentation
Cratering
Shear Bands

A

20. ABSTRACT (Continue on reverse side if necessary and identify by block number)

Steel target plates impacted at hypervelocities by small projectiles of various sizes, shapes, and materials were examined metallographically. The purpose was to provide a physical basis for the development of theories that can be used to predict and interpret hypervelocity impact phenomena and to design projectiles that are more effective in producing backface armor fragmentation.

DD FORM 1 JAN 73 1473
EDITION OF 1 NOV 65 IS OBSOLETE

UNCLASSIFIED
SECURITY CLASSIFICATION OF THIS PAGE (When Data Entered)

DN

332 500

19. KEY WORDS (Continued)

20 ABSTRACT (Continued)

The relative importance of projectile momentum and kinetic energy on target damage is discussed. Several observed effects of projectile material on the extent of back surface damage are explained by the relative high pressure shock impedances of projectile and target. The effect of additional momentum delivered to the target when the projectile vaporizes was studied in a single experiment. Postulated blow-off momentum appears to result in a small increase in target damage, but more data are required before conclusions regarding the effect of projectile vaporization can be drawn.

Scaling considerations of the MERDC/NRL experiments suggest that 1- to 2-kg spheres traveling at 5 km/sec would be required to spall 8-inch-thick steel armor. The mass ejected from the back surface may be 25 times that of the projectile.

Differences in front surface damage morphology produced by low shock impedance and equi- or high impedance projectiles are explained by the tendency of equi- or high impedance projectiles to penetrate and low impedance projectiles to reverse their direction during impact. This is thought to change the direction of the maximum shear stresses produced in the targets and cause the observed changes in shear band orientation.

The number and total length of shear bands or associated shear band cracks do not appear strongly dependent on projectile velocity, but are significantly greater for nylon and polycarbonate than for steel projectiles. No shear bands were observe. in the single target specimen of austenitic steel, although the cracking pattern was similar in all respects to those specimens that exhibited shear bands.

Metallographic examination of back surface target fragments showed that shear banding occurs at the back surface to a limited extent.

ACKNOWLEDGMENTS

The authors appreciate the enthusiasm and interest of J. W. Bond, Jr., and the skillful metallographic work of D. Petro.

CONTENTS

LIST OF ILLUSTRATIONS

LIST OF TABLES

I INTRODUCTION

The Army is evaluating the feasibility and effectiveness of hypervelocity weapons under the Hypervelocity Impact Technology (HIT) program. One of the main objectives of the program is to understand the effects of projectile size, shape, configuration, and material(s) on target back surface fragmentation. In support of this objective the Mobility Equipment Research and Development Center (MERDC) has performed hypervelocity impact experiments on rolled homogeneous steel armor plate using the Naval Research Laboratory gas gun facility. Various projectile materials and geometries were investigated.

Under a recent contract with MERDC, SRI performed metallographic and fractographic examinations of the impacted specimens to identify and describe physical changes that occurred in the steel. The present contract extended this research and directed special attention to (1) the relative importance of impact (and blow-off) momentum and kinetic energy to target damage, (2) differences in crater morphology and near-crater fracture patterns for different projectile materials, (3) the influence of projectile size and configuration, (4) the occurrence of shear banding, and (5) back face spall and fragmentation. The purpose of this research was to provide a physical basis for the development of theories that could be used to predict and interpret hypervelocity impact phenomena and to design projectiles that are more effective in producing back face armor fragmentation.

II EFFECT OF PROJECTILE PARAMETERS ON TARGET DAMAGE

Twenty-two hypervelocity impact specimens were received during the contract period (June 1974 through May 1975) and examined metallographically. Impact conditions and damage parameters are given in Table I. These investigations supplement those on previously obtained specimens, listed in Appendix A of Reference 1.

The fracture damage in steel plates produced in these and in previously reported impact experiments using projectiles having shock impedances much lower than, equal to, and considerably above that of the steel targets was evaluated quantitatively. Plots were made of back surface bulge against projectile momentum and kinetic energy for spheres of similar size but of different material (Figures 9 and 10 in Reference 2).

Figure 11 of Reference 2 shows the effect of sphere size on macro-fracture diameter. Three observations may be made from these figures:

(1) Impact velocity is important. At higher velocities, small increases in velocity result in large increases in damage. For example, in Reference 1 it was reported that for nylon spheres of 0.953 cm diameter impacting 1.27 cm steel plates, incipient spall damage occurs at impact velocities around 4 km/sec, and production of a hole through the plate by means of ejection of back surface material occurs at impact velocities around 5.5 km/sec.

(2) For equisized projectiles, the projectile kinetic energy to produce a given amount of back surface damage is not a strong function of projectile material (see Figure 9 in Reference 2).

(3) For equisized projectiles, the projectile momentum to produce a given amount of back surface damage is a strong function of projectile material (see Figure 10 in Reference 2).

These three observations may be at least partially explained on the basis of projectile shock Hugoniot equation of state alone. The effect of the Hugoniots alone can be illustrated by considering the more simple case of flat impacts of plates rather than spheres. Figure 1 shows the

Table I

IMPACT CONDITIONS AND TARGET DAMAGE PARAMETERS FOR ADDITIONAL HYPERVELOCITY IMPACT EXPERIMENTS

Experiment Number	Projectile					Target									
	Material	Diameter (cm)	Mass (gm)	Velocity (km/sec)	Kinetic Energy (cal)	Momentum (kg-m/sec)	Thickness (cm)	D_c (cm)	P (cm)	V (ml)	Crater/ Spall *	δ (cm)	D_s (cm)	D_{cs} (cm)	T (cm)	W (gm)
1-917	Nylon	0.953	0.519	6.38	1740	1.42	(a)				B/C					
1-921	SP-2 into ESR	(i)	3.58	~6.6	12980	19.7	(o)	4.48			C/B(d)	-	2.10	-	0.61	4.33
1-922	Nylon	0.953	0.519	5.24	1700	2.72	(b)	1.6	0.48		A/B	0.124	0.961	0.31	0.31	2.4
1-923	Steel	0.714	1.49	4.62	3800	6.86	2.54	2.4	1.26		A/B	0.23	1.97	0.44	0.64	2.33
1-924	Nylon	0.953	0.515	5.32	1740	2.74	(c)	1.68	0.53		B/A	0	2.18	1.02	0.39	0.77
1-925		n.s.														
1-926		n.s.														
1-927	Nylon	0.953	0.520	5.21	1690	2.71	(f)									
1-928	Nylon	0.953	0.520	5.20	1680	2.70	(g)									
1-929	Nylon	0.953	0.520	5.23	1690	2.72	(h)									
1-930	2017 Al	0.635	1.27	5.3	4370	6.73	2.54									
1-931	Steel	0.318	0.690	5.4	2440	3.77	(j)									
1-932		(i)	4.11	5.3	11800	18.6	2.54									
1-933		(j)	3.23	5.3	11860	18.7	2.54(h)									
1-934		(j)	3.60	5.3	12110	19.1	(m)									
1-938		(n)	4.03	~4.9	11550	18.7	2.54									
1-939			4.00	4.9	11490	19.6	2.54									
1-941			3.51	4.9	10080	17.2										
6-641	Lead	0.470	0.572	5.7	2220	3.26	2.54	1.88	1.02	1.7						
6-643	Nylon		n.s.													
NOL #1		(o)	3.1	6.26	14540	19.4	2.54									

* These designations are defined in Reference 1.

(a) 1.27-cm-thick armor with 0.953-cm plexiglass backing.
(b) 1.27-cm-thick armor with 0.953-cm plexiglass with 1.27-cm armor.
(c) 2.54-cm armor with 0.953-cm plexiglass backing.
(d) Four spall fragments.
(e) 2.70-cm-thick ESR steel.
(f) 2.54-cm-thick 7039-T6 aluminum.
(g) 2.54-cm-thick armor with 1.27-cm-thick polycarbonate backing.
(h) 1.27-cm-thick soft ESR steel.
(i) SP-2 projectile cylinder 1.3 cm dia x 1.3-cm-long.
(j) 1.27-cm-dia polycarbonate cylinder containing central steel core.
(k) Fort Belvoir MS soft steel.
(l) 1.27-cm-thick ESR steel.
(m) Two 1.27-cm-thick steel plates placed 2.54-cm apart.
(n) Tungsten carbide disk in polycarbonate.
(o) Polycarbonate cylinder 1.3-cm diameter and 1.6-cm long with small steel cap.

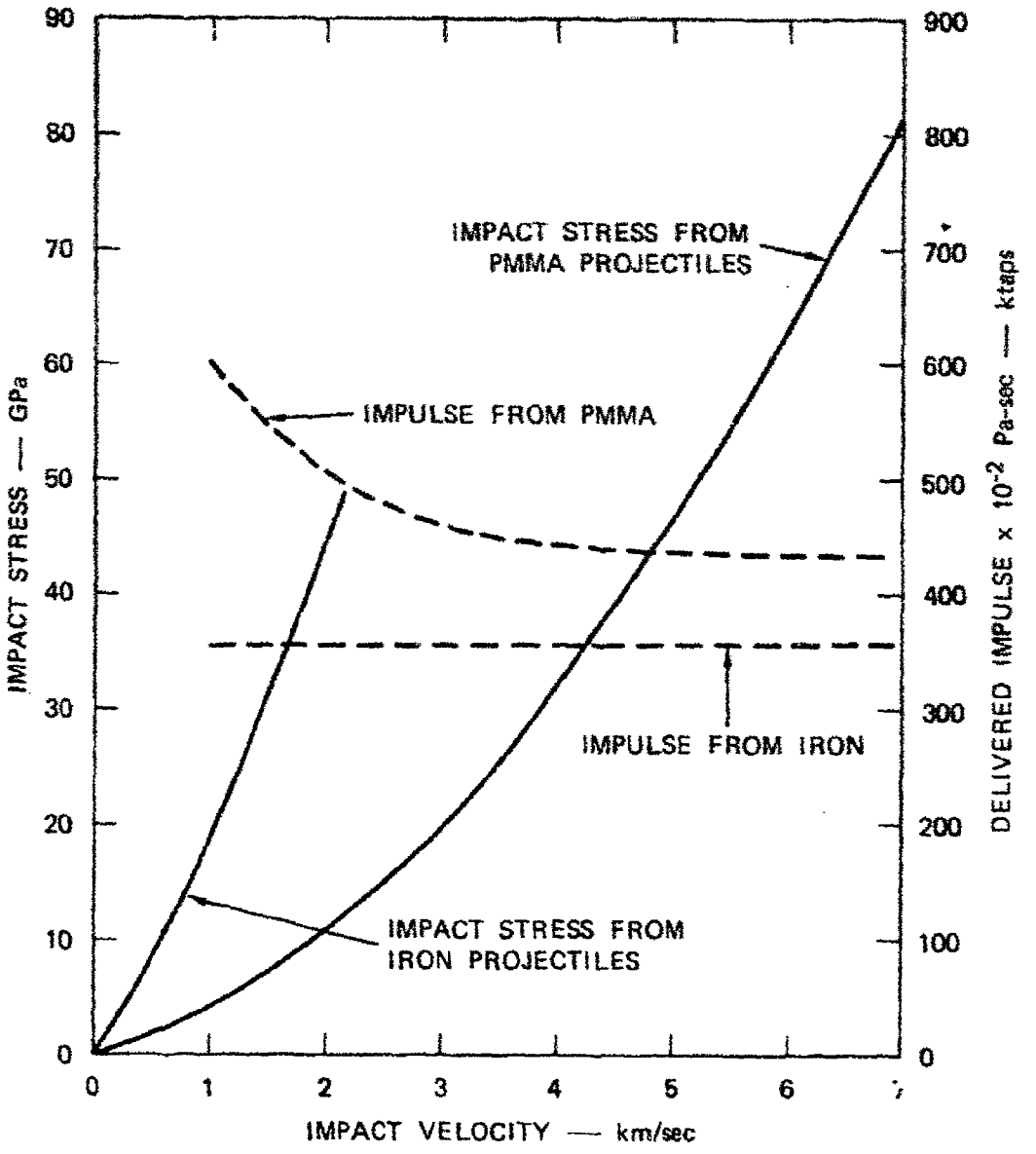

FIGURE 1 VARIATION OF IMPACT STRESS AND DELIVERED IMPULSE WITH IMPACT VELOCITY FOR FLAT PLATE IMPACT OF PMMA AND IRON AT EQUAL MOMENTA

impact stresses and delivered impulses (integral of the pressure history at the interface) for polymethylmethacrylate (PMMA) and iron plates impacting steel targets as a function of impact velocity but at a constant incoming projectile momentum of 0.356 MPa-sec. Figure 2 plots the same quantities for a constant incoming projectile kinetic energy of 5.7×10^6 joules/m^2. The Hugoniot data used to compute the curves of Figures 1 and 2 were taken from Reference 3. It can be seen that, for both constant momentum and constant kinetic energy projectiles, the effect of increasing the material shock impedance (at high pressures) is to increase the peak impact stress but to decrease the delivered impulse. Furthermore, increasing the impact velocity beyond about 3 km/sec causes rapid increases in the impact stresses but results in constant or slowly decreasing delivered impulses.

Thus, considerations of Hugoniots alone suggest that small, fast projectiles should be more damaging than larger, slower ones with the same momenta or kinetic energies, in agreement with the first observation above.

The second observation above may be inferred from Figure 2. PMMA and iron projectile plates of identical sizes and kinetic energies have an impact velocity ratio given by

$$\frac{v_{PMMA}}{v_{iron}} = \left(\frac{\rho_{iron}}{\rho_{PMMA}} \right)^{\frac{1}{2}} \cong 2.5$$

Thus, if the iron projectile impacts at 3 km/sec, for example, the corresponding PMMA projectile must impact at 7.5 km/sec. Figure 2 then shows that the impact stresses and the delivered impulses for the two projectiles will be similar. Thus it is expected that the two projectiles would cause similar amounts of target damage.

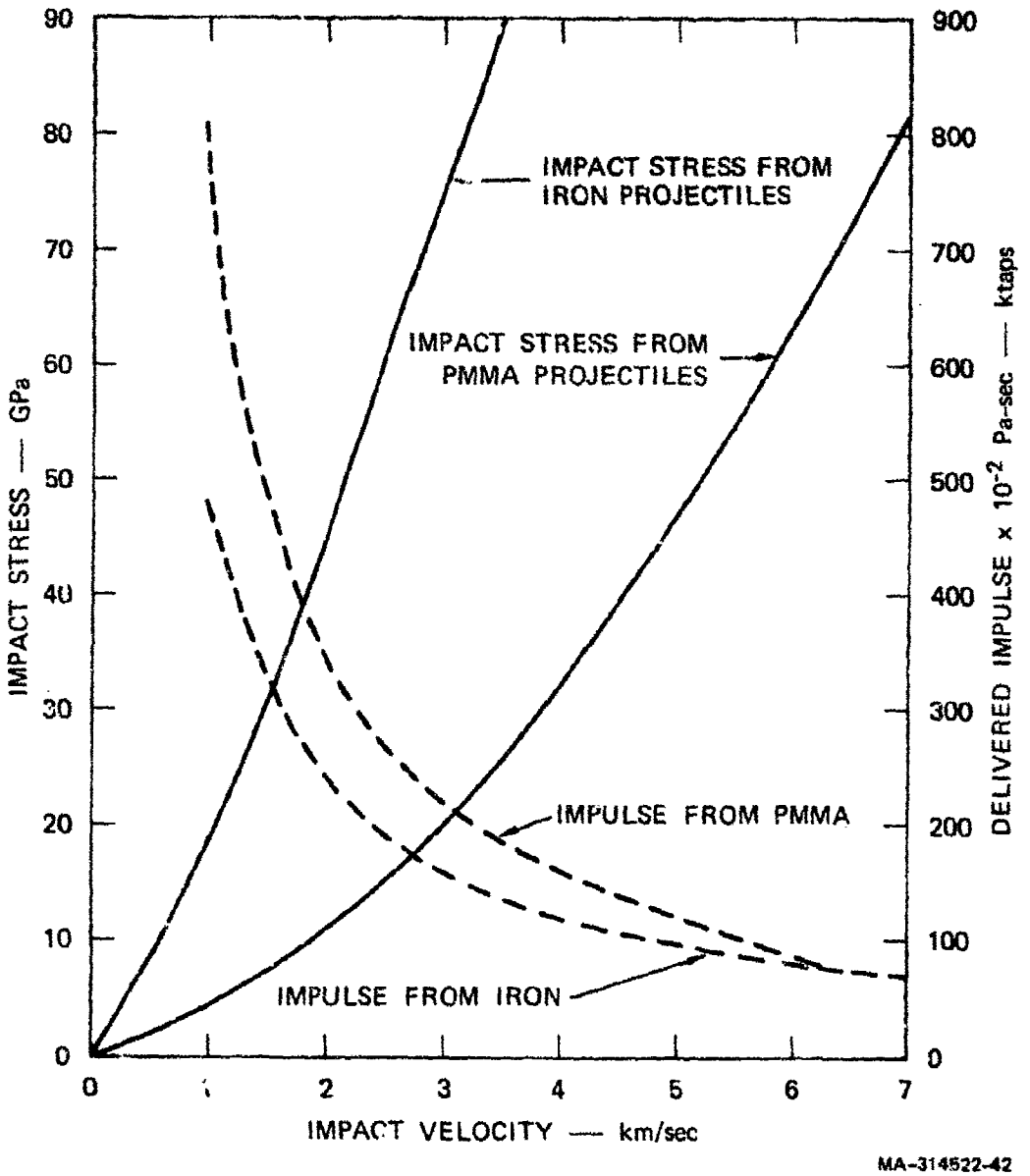

FIGURE 2 VARIATION OF IMPACT STRESS AND DELIVERED IMPULSE WITH IMPACT VELOCITY FOR FLAT PLATE IMPACT OF PMMA AND IRON AT EQUAL KINETIC ENERGIES

The third observation above may be similarly inferred from Figure 1. PMMA and iron projectiles of identical sizes and momenta have an impact velocity ratio given by

$$\frac{v_{PMMA}}{v_{iron}} = \frac{\rho_{iron}}{\rho_{PMMA}} \cong 6.5$$

Thus, if the iron projectile impacts at 1 km/sec, for example, the corresponding PMMA projectile must impact at 6.5 km/sec. Figure 1 then shows that both the impact stress and delivered impulse will be greater for the PMMA projectile. Therefore, the target damage should be greater for the low-impedance projectile, as observed.

It thus appears that shock Hugoniot considerations alone explain some of the observed effects of projectile material. However, there are several limitations to the above arguments. First, for impacting spheres or cylinders, the early arrival of relief waves from the lateral boundaries of smaller projectiles should eventually counteract the effects of the higher impact stresses. Second, damage mechanisms usually become impulse dominated for very short duration loads,[4-8] suggesting that the damage should eventually "saturate" for hypervelocity impacts of constant delivered impulse. A third complication is the possible effects of vaporization and "blow-off" of the projectile material. Thus, shock Hugoniot considerations must be supplemented by better understanding of the roles played by phase changes and projectile geometry before the effects of projectile material properties on the target damage can be understood completely.

III EFFECT OF BLOW-OFF MOMENTUM

As discussed previously, the momentum delivered to a target by an impinging projectile determines to a large extent the damage inflicted on the target. Additional momentum could be delivered to the target if the projectile vaporized on impact, although it is not clear that this (so called) "blow-off momentum" would be significant. To investigate the effect of blow-off momentum, SRI suggested that identical steel targets be impacted by projectiles of iron and lead of such sizes and velocities to produce approximately the same stress histories in the targets. The main difference in the two experiments would then be that the lead projectile should receive enough shock energy to cause it to vaporize, whereas the iron projectile should not vaporize. The conditions for identical stress histories are given in the Appendix along with the calculations. Note that the lead projectile requires only about one-fifth of the kinetic energy of the iron projectile to produce the same impact stress history.

The lead sphere experiment was carried out by W. W. Atkins and M. Persechino at the NRL impact facility. Unfortunately, however, the corresponding recommended iron impact experiment was not performed during the contract period. Three previous impact experiments (1-906, 1-909, and 1-911) had been made with steel spheres of approximately the right size, mass, and velocity, but unfortunately were performed on 1.27-cm-thick rolled homogeneous armor instead of 2.54-cm-thick material. In all three cases the back surface spall section was completely detached, and so direct comparisons of target damage with that produced by the lead sphere were not possible. Thus, conclusions concerning the effect of blow-off on target damage must await a comparable experiment with a steel sphere.

A steel sphere of similar velocity, although of somewhat greater mass than the lead sphere, had been impacted against a 2.54-cm-thick steel plate and provided an opportunity to compare the damage. By

reason of its higher mass, the kinetic energy and momentum of the steel projectile were about 20% larger than for the lead projectile.

Impact conditions and damage parameters are given in Table II. The shock energy for the lead impact was about 1000 cal/gm, well above the assumed lead sublimation energy of 220 cal/gm.[9*] The shock energy for the steel impact was also 1000 cal/gm, but considerably below the assumed iron sublimation energy of 1770 cal/gm.[9] Thus the lead was expected to vaporize and deliver additional momentum to the target.

Qualitatively, the target damage produced by the lead sphere was much like that produced by steel spheres and unlike that produced by nylon and polycarbonate. That is, the crater was hemispherical rather than conical, and shear bands and associated cracks ran upward rather than downward. In addition, the typically observed cavitation beneath the crater was evident. The $\alpha \rightleftarrows \epsilon$ phase transformation zone was large, extending to a depth of about 4 mm below the crater floor, and the crater floor itself consisted of a thick layer (about 0.6 mm) of white-etching material suggestive of martensite.

The lead sphere produced slightly more damage than the steel sphere. Table II shows that the crater in the lead impacted specimen was somewhat wider and about 12% deeper than in the steel impacted specimen. Furthermore, the boundary of the hemispherical $\alpha \rightleftarrows \epsilon$ phase transition region (i.e., the 130-kbar isobar) was 1.5 cm below the original surface for the lead impact and 1.4 cm for the steel. Finally, the back surface bulge produced by the lead sphere was slightly greater than that from the steel sphere, although the spall width was somewhat less. Thus the lead impact appeared slightly more damaging even though the momentum and kinetic energy of the lead sphere were 15% to 20% lower than for the steel sphere. The lack of a more dramatic increase of

*Large uncertainties exist in the sublimation energies appropriate under these dynamic loading conditions.

Table II

IMPACT CONDITIONS AND DAMAGE PARAMETERS FOR SIMILAR EXPERIMENTS WITH A LEAD AND A STEEL SPHERE

PROJECTILE							TARGET								
Experiment Number	Shape and Material of Projectile	Diameter (cm)	Mass (g)	Velocity (km/sec)	Kinetic Energy (cal)	Momentum (kg-m/sec)	Thickness (cm)	Crater Diameter (cm)	Crater Depth (cm)	Crater Volume (ml)	Crater Spall	Back Face Bulge (cm)	Position of Spall (cm)	Thickness of Spall Layer (cm)	Width of Spall (cm)
6-641	ead sphere	0.47	0.5717	5.7	2218	3.26	2.54	1.68	1.09	1.7	A	0.17			2.28
1-857	teel sphere	0.556	0.699	5.629	2649	3.93	2.54	1.8	0.97	n.a.	A/B	0.15	2.1	0.57	2.5

damage indicates that the contribution of blow-off momentum was small. However, the magnitude of blow-off effects might be expected to increase at higher velocities.

IV CONDITIONS NECESSARY TO SPALL 8-INCH-THICK ARMOR

The Sandia damage calculations for hypervelocity impact of steel with nylon assumed rate-independent constitutive relations;[10] hence, they should scale linearly to any armor thickness. This assumption is borne out by the limited data available from MERDC-NRL experiments.[1] Scaling these data for 1/2- and 1-inch armor indicates that spallation of 8-inch-thick armor could be produced by impact of spheres weighing 1 to 2 kilograms impacting at 5 km/sec. Scaling up the data of Ref. 1 suggests that the mass ejected from the back surface may be 25 times that of the projectile.

V EFFECTS OF PROJECTILE MATERIAL ON CRATER MORPHOLOGY AND NEAR-CRATER FRACTURE PATTERNS

It was noted in the previous work that low impedance projectiles produced conical craters and downward-running near-crater shear bands, whereas equal or high-impedance projectiles produced hemispherical craters and upward-running near-crater shear bands.

A possible explanation for the two kinds of cracking patterns involves conditions at the interface between target and projectile. Steel and tungsten carbide projectiles have shock impedances equal to or greater than that of the target. Thus, as they advance into the target, they tend to pull with them the target material at the interface. The interface target material is, thus, subjected to large shearing stresses that are relieved when a shear band or a crack, or both, form and propagate. Maximum shear stress trajectories and, hence, the shear bands and cracks are oriented in the observed cone configuration because of the downward thrust of the steel and tungsten carbide spheres.

The downward and outward configuration of cracks resulting from nylon, Lexan, titanium, glass, and Al_2O_3 impacts may be attributable to the tendency of lower shock impedance materials to reverse their direction during impact, thus causing the subsequent flow of projectile material upward and outward. In this case, the frictional forces on the target material from the flowing projectile mass pull the peripheral material in the opposite sense. Here the trajectories of maximum shear stress in the target and the shear bands and cracks lie in an inverted cone pattern.

Maurer and Rinehart[11] discussed the shapes and mechanism of formation of craters and crater-associated cracks produced in rocks by similar small steel spheres at lower velocities (to about 3 km/sec). They found that as the projectile penetrated the rock, fractures

apparently initiated in a steplike fashion and propagated along planes of maximum shear, defined by a logarithmic spiral

$$r = r_o \exp \left[\pm \theta \tan \left(45^\circ + \frac{\mu}{2}\right)\right]$$

where r is a radius vector of the spiral, r_o the distance from the point of application of the load to the intersection of the logarithmic spiral and the horizontal boundary, θ the polar angle from the nearest surface, and μ the angle of internal friction.

Maurer and Rinehart[11] noted that the spacing between subcrater fractures was constant and explained this observation by assuming that a constant impulse was required to initiate each fracture. Letting the distance between two successive fractures be Δs, they showed that the time the projectile acts on this portion of the crater is $\Delta t = \Delta s/V$, where V is instantaneous projectile velocity. Since the instantaneous force resisting the projectile was assumed proportional to the projectile velocity, $F = kV$, the impulse I is given by $I = F\Delta t = k\Delta s$ and is thus constant. This explanation may also apply to the fracture patterns observed in the craters of the steel targets.

VI SHEAR BANDS

One of the tasks included in this work involved providing a more detailed account of "adiabatic shear bands." Two questions in particular were "Do they form adiabatically?" and "Is the material within the bands martensite?" This section seeks to answer these questions, then discusses attempts to correlate shear band activity with projectile parameters.

The adiabatic shear bands referred to in Reference 1 were thin bands of high hardness, visible on polished and etched cross sections of steel targets extending inward from the crater walls and also connecting individual microfractures in the immediate subcrater region. The bands appeared white when etched in 5% nital and contrasted sharply with the dark etching background metal. The bands were typically a few microns in width, often branched, and generally acquired fractures along their lengths. That these bands experience intense shearing strains is obvious from micrographs such as Figure 9 in Reference 1, which show large displacements in the rolling lines of the target plates.

Thus these bands can safely be called shear bands, but the addition of the adjective "adiabatic" is not as straightforward to justify. The term "adiabatic shear band" probably originated in a paper published in 1944 by Zener and Hollomon[12] who were among the first to report the phenomenon, and whose postulated mechanism remains as the most likely one. Their mechanism in essence is as follows: when a body is strained at high rates, necessary displacements within the body cannot be accommodated in a uniform manner. Instead shear instabilities develop at discrete sites in the body, and these instabilities grow because of local thermal softening. The plastic work in the shear site is converted into heat that cannot be dissipated effectively into the surrounding material within the short times involved. Hence the temperature rises in the local volume where the instability occurred. Since the flow stress of most metals

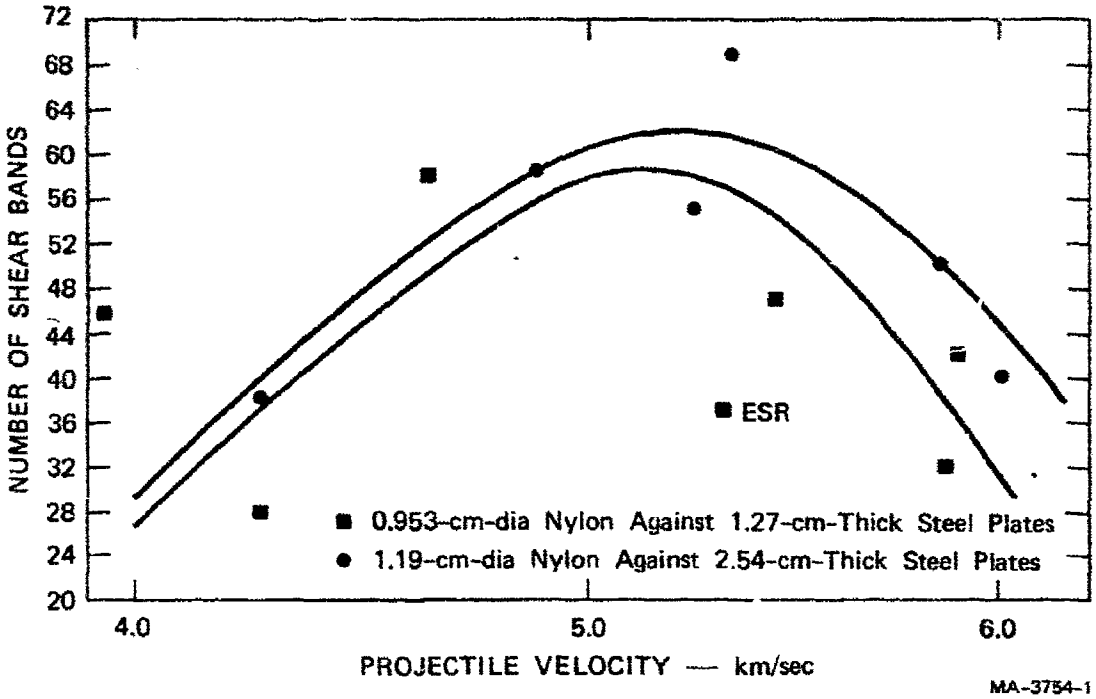

FIGURE 3 EFFECT OF NYLON PROJECTILE VELOCITY ON NUMBER OF NEAR CRATER SHEAR BANDS IN IMPACTED STEEL PLATES

decreases at elevated temperatures, it becomes easier for the next increment of plastic flow to occur in the heated material rather than elsewhere. The additional increment of plastic flow results in additional local heating and so the process continues, confining slip almost exclusively to narrow bands, which propagate on planes of maximum shear stress through the specimen.

In the strict thermodynamic sense, however, the term 'adiabatic" is hard to justify. Adiabatic means no gain or loss of heat. The process may be nearly adiabatic as slip occurs and drives the temperature up, but most certainly nonadiabatic conditions exist as heat is conducted away by the surrounding metal at later times. The observed austenite to martensite transformation within shear bands in steel indicates that heat is lost at very rapid rates. Thus total adiabaticity is a thermodynamic ideal, and the degree of shear adiabaticity must vary with the material and the loading rates.

Similarly, since the ability to form martensite depends on the thermal history, the answer to the second question depends on the material and the loading rates. To obtain positive confirmation that the material within the shear bands observed in Reference 1 transformed to martensite would require a detailed look at the structure and carbon distribution within the bands with x-ray diffraction and transmission electron microscopy. Such an investigation has been performed on a 1% C, 1% Cr steel by Wingrove,[13] who concluded from the results that the structure is martensite. While this does not prove that the bands in MIL-S-12560B were transformed to martensite, it does show that such is probable.

Quantitative analyses of the shear banding and cracking activity near the impact craters was attempted. The shear bands and cracks extending inward from the crater surfaces of approximately 35 specimens impacted with nylon, polycarbonate, and steel spheres were counted and measured.

Specimens impacted with nylon spheres contained typically 40 to 60 shear bands per specimen, roughly one-third of which were cracked. The cracked shear bands tended to correlate one-to-one with the cusps on the terraced crater surface. Between adjacent cracked shear bands (cusps) were several (usually two) finer uncracked shear bands having shapes similar to the larger cracked bands.

The variation of number of shear bands with impact velocity is shown in Figure 3. No decisive trend was apparent for velocities between 4 and 6 km/sec, although the data suggest a maximum near 5 km/sec.

The correlations were made, assuming the shear strain associated with a band to be a constant. This was not the case, however. Fine bands with small shear displacements and coarse bands with large displacements were commonly observed on the same specimen, and, moreover, the width of a given band varied along its length. The general tendency was for the transformed width to be large and the deformation width to be small near the band origin, whereas the transformed width became progressively smaller and then vanished further from the loading site. The width of the deformed zone correspondingly increased and eventually went over to homogeneous deformation. However, the scope of the work precluded collecting statistical data on shear band widths.

No shear bands were observed in the single target specimen of austenitic steel. Although transformed bands were not expected because the $\alpha \rightleftarrows \gamma$ phase transformation cannot occur, we expected deformation bands because of the similar loading conditions. However, no severe local deformations of the grains could be detected metallographically, and deformation appeared homogeneous. The cracking pattern, on the other hand, was similar to that observed in the MIL-S-12560B, and 15 cracks were observed extending downward and outward from the crater floor in the same manner as when shear banding occurs.

Correlations between shear band activity and projectile velocity, material, and size were sought by constructing plots of shear band number, density, and total length, versus impact velocity for spherical projectiles of several materials and sizes. No clear trend was indicated.

Compared with nylon spheres, fewer instabilities, typically 10 to 25, were observed in specimens impacted with steel spheres. However, these data were for spheres of either smaller diameter (0.554-0.714 cm; cf nylon diameters of ~ 1 cm) or lower velocities (~ 2km/sec; cf nylon velocities of ~ 5 km/sec). Usually 10 to 15 instabilities were produced by small diameter, high speed projectiles (0.5-0.7 cm-diameter, 5 km/sec) whereas significantly more (about 25) were typically produced by larger, slower projectiles (~ 1 cm diameter, 2 km/sec). The percentage of shear bands that cracked was higher for steel sphere impact than for nylon, and increased with velocity. Around 2 km/sec, approximately 50% of the shear bands cracked; at about 5 km/sec 70% to 90% were cracked.

It was difficult to investigate shear banding trends for targets impacted by liquid-filled polycarbonate projectiles because of the meager reliable data. Of the 14 experiments performed, four gave evidence of leakage during flight, three used materials other than polycarbonate, water, and rolled steel, and two were of cylindrical geometry. The available information suggests, however, that the shear banding/cracking behavior is similar to that produced by nylon spheres, i.e., 40 to 60 bands, roughly one-third of which are cracked.

VII BACK SURFACE EJECTA

Back surface ejecta from two experiments were examined with a microscope. The "scab" from the Experiment 1-881 and several of the nine fragments recovered from Experiment 1-878 were mounted in clear plastic mounting compound and ground down on abrasive paper. These cross sections were then polished and etched to reveal the internal features. These fragments were examined with a microscope to deduce the mechanism of back surface fragmentation. The role of shear bands was of special interest.

A cylindrical "scab" of material, approximately 4 cm in diameter by 0.5 cm thick, was ejected from the back surface of specimen 1-881 in essentially one piece and recovered. This piece was sectioned by cutting, mounted in clear plastic, polished, and etched.

No evidence of transformed shear bands was found on the periphery of the scab. This is in agreement with observations made previously on specimens that had suffered back surface mass loss. Adiabatic shearing did occur, however, in localized regions on the fracture surface. The fracture surface forms by the nucleation, growth, and coalescence of microfractures. The last step, coalescence, requires considerable shearing as microvoids grow together and nonplanar macrocracks (coalesced microvoid clusters) join up. Thus very small white etching regions of high hardness were observed at occasional sites on the fracture surface (Figure 4a). This behavior has also been observed in one-dimensional strain plate slap experiments.

Hardness measurements were made on the white-etching transformed material and also on the adjacent material. Vickers Hardness Numbers (200-gram load) of the transformed material were typically 750 to 800 (R_c 62-65), whereas the adjoining areas were softer than the base metal at 270 to 300 (R_c 26-30) (see Figure 4b).

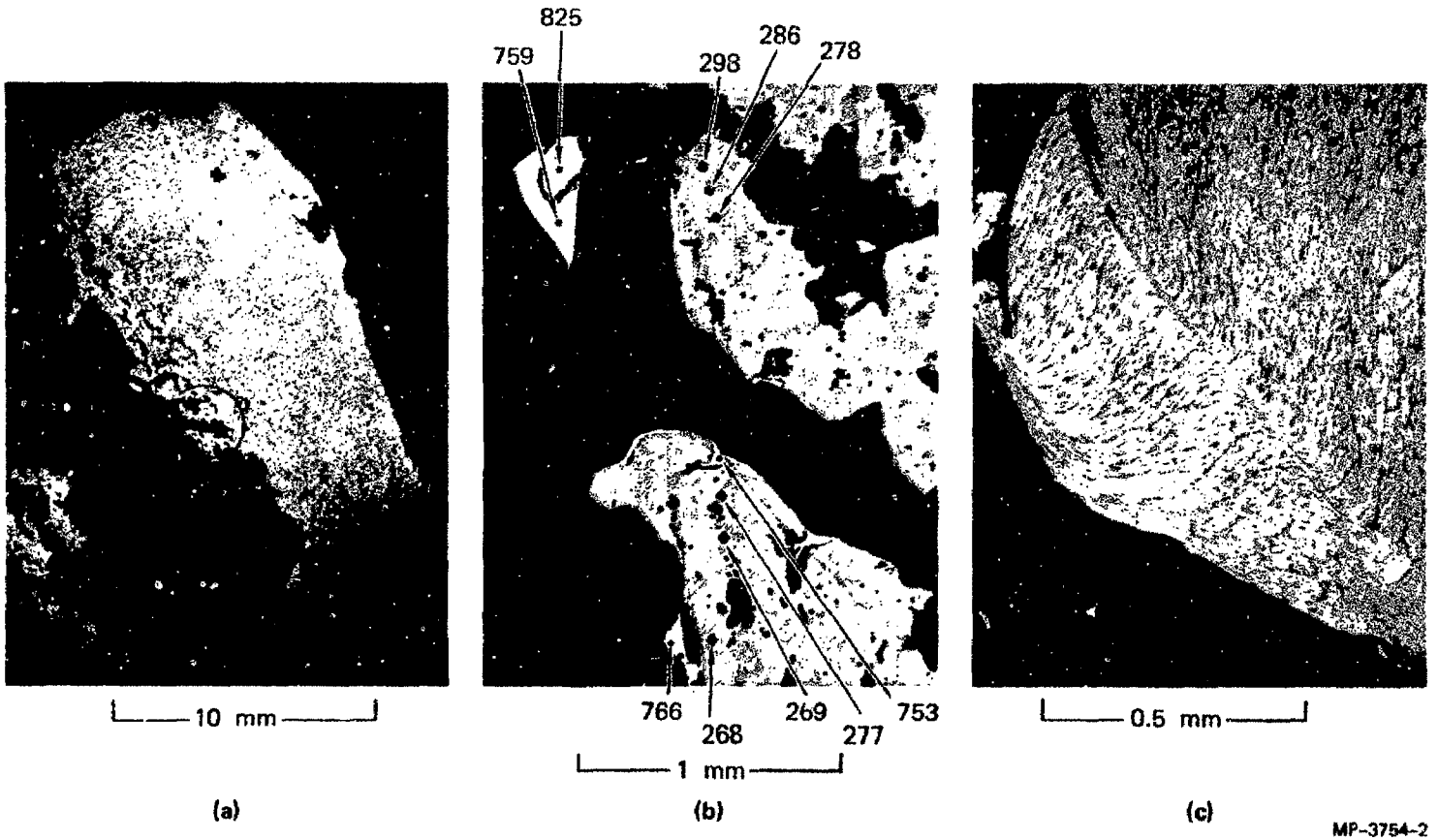

FIGURE 4 (a) POLISHED AND ETCHED CROSS SECTION THROUGH BACK SURFACE SCAB FROM SPECIMEN 1-831
(b) CLOSE-UP VIEW OF REGION NEAR FRACTURE SURFACE [CIRCLED IN (a)] SHOWING VARIATIONS IN VICKERS HARDNESS
(c) DEFORMATION SHEAR BANDS IN A NEAR SURFACE FRAGMENT FROM EXPERIMENT 1-878

Larger shear bands of the deformation type (not transformed) were observed on occasion on polished and etched cross sections of the fragments from Experiment 1-878. Figure 4c shows two such bands, one of which has become a fracture surface and fragment boundary; the other has begun to fail.

REFERENCES

1. D. A. Shockey, D. R. Curran, P. S. De Carli, J. P. Wilhelm, and D. Petro, "Physical Changes Occurring in Armor Steel Under Hypervelocity Impact," Final Report U.S. Army BRL, Aberdeen Proving Ground, Md., on Contract DAAD05-73-C-0025, March 1974.

2. D. A. Shockey, D. R. Curran, and P. S. De Carli, "Damage in Steel Plates from Hypervelocity Impact: Part I Physical Changes and Effects of Projectile Material," to be published in J. Appl. Phys. 1975.

3. R. G. McQueen, S. P. Marsh, J. W. Taylor, J. N. Fritz, and W. J. Carter, "The Equation of State of Solids from Shock Wave Studies," in High Velocity Impact Phenomena, R. Kinslow, ed. (Academic Press, New York 1970) Chapter 2, p. 294.

4. L. Seaman, T. W. Barbee, Jr., and D. R. Curran, "Dynamic Fracture Criteria of Homogeneous Materials," Technical Report No. AFWL-TR-71-156, Air Force Weapons Laboratory, Kirtland Air Force Base, New Mexico (December 1971).

5. T. W. Barbee, Jr., L. Seaman, R. Crewdson, and D. Curran, "Dynamic Fracture Criteria for Ductile and Brittle Metals," Journal of Materials, JMLSA, Vol. 7, No. 3, 393-401 (September 1972).

6. D. A. Shockey, L. Seaman, and D. R. Curran, "Dynamic Fracture of Beryllium Under Plate Impact and Correlation with Electron Beam and Underground Test Results," Technical Report No. AFWL-TR-73-12, Air Force Weapons Laboratory, Kirtland Air Force Base, New Mexico (January 1973).

7. D. R. Curran, D. A. Shockey, and L. Seaman, J. Appl. Phys. 44, 9, 4025-4038 (September 1973).

8. G. R. Abrahamson, and H. E. Lindberg, Proc. of Dynamic Response of Structures Symp., Stanford University, Stanford, California, June 28-29, 1971, p. 31-53.

9. D. J. Kohn, "Compilation of Hugoniot Equations of State," Tech. Report No. AFWL-TR-69-38, Air Force Weapons Laboratory, Kirtland AFB, New Mexico, April 1969.

10. L. D. Bertholf, L. D. Buxton, B. J. Thorne, R. K. Byers, A. L. Stevens and S. L. Thompson, "Damage in Steel Plates from Hypervelocity Impact," Part II Numerical Results and Spall Measurement," to be published in J. Appl. Phys. 1975.

11. W. C. Maurer and J. S. Rinehart, "Impact Crater Formation in Rock," J. Appl. Phys. 31, 1247 (1960).

12. C. Zener and J. M. Holloman, J. Appl. Phys. 15, 22 (1944).

13. A. L. Wingrove, "A Note on the Structure of Adiabatic Shear Bands in Steel," Technical Memorandum 33, Australian Defence Scientific Service, Defence Standards Laboratories, Department of Supply, Maribyrnong, Victoria, March 1971.

Appendix

CALCULATION OF DIAMETER OF LEAD PROJECTILE TO GIVE SAME IMPACT DURATION AS AN IRON PROJECTILE

Iron and lead have Hugoniots that lie close together in the P, u plane, particularly in the high pressure region. However, the shock velocity in lead is lower, thus requiring smaller lead projectiles to give the same shock reverberation time as for an iron projectile at the same impact pressure. The calculations here are for impacting plates rather than for spheres. This will cause an error because spheres will suffer less compaction. However, the reverberation times should be roughly correct.

Choose an impact velocity of 5 km/sec. Since lead and iron have similar Hugoniots in the P, u plane, the impact pressure for an iron target will be about 1500 kbar in both cases. At this pressure:

Shock velocity for iron = U_s^{Fe} = 12.4 mm/μsec

Shock velocity for lead = U_s^{Pb} = 5.7 mm/μsec

The Hugoniot pressure-density relation is

$$P_H = C\left(\frac{\rho}{\rho_o} - 1\right) + D\left(\frac{\rho}{\rho_o} - 1\right)^2 + S\left(\frac{\rho}{\rho_o} - 1\right)^3$$

Thus

$$\left(\frac{dP_H}{d\rho}\right)^{1/2} = \left\{ \frac{C}{\rho_o} + \frac{2D}{\rho_o}\left(\frac{\rho}{\rho_o} - 1\right) + \frac{3S}{\rho_o}\left(\frac{\rho}{\rho_o} - 1\right)^2 \right\}^{1/2}$$

The Lagrangian sound speed is given approximately by

$$C_L \simeq \frac{\rho}{\rho_o} \left(\frac{dP_H}{d\rho}\right)^{\frac{1}{2}}$$

We next compute C_L for iron and lead at 1500 kbar:

Material	ρ_o	$\frac{C}{\rho_o}$	$\frac{2D}{\rho_o}$	$\frac{3S}{\rho_o}$	$(\frac{\rho}{\rho_o} - 1)$	$(\frac{\rho}{\rho_o} - 1)^2$	$(\frac{dP_H}{d\rho})^{1/2}$	C_L
Iron	7.85	12.9×10^{10}	108×10^{10}	195×10^{10}	0.45	0.20	10.0	14.5
Lead	11.4	4.4×10^{10}	8.8×10^{10}	53×10^{10}	0.75	0.56	5.5	9.6

where ρ_o is in gm/cm^3, C/ρ_o, $2D/\rho_o$, and $3S/\rho_o$ are in ergs/gm and the remaining quantities are in mm/μsec.

The reverberation time is given by

$$\Delta t = \frac{\Delta h}{U_s} + \frac{\Delta h}{C_L} ,$$

where Δh is the original projectile diameter (or plate thickness under our flat plate assumption).

Thus

$$\Delta h = \frac{\Delta t}{(\frac{1}{U_s} + \frac{1}{C_L})}$$

If the iron projectiles have a diameter of 11.5 mm, then

$$\Delta t_{Fe} = \frac{11.5 mm}{12.4 \frac{mm}{\mu sec}} + \frac{11.5 mm}{14.5 \frac{mm}{\mu sec}} = 0.95\ \mu sec + 0.79\ \mu sec = 1.7\ \mu sec$$

Thus, for the lead to have the same Δt, we have:

$$\Delta h_{Pb} = \frac{\Delta t_{Fe}}{\frac{1}{U_s^{Pb}} + \frac{1}{C_L^{Pb}}} = \frac{1.7\ \mu sec}{\left(\frac{1}{5.7} + \frac{1}{9.6}\right) \frac{\mu sec}{mm}} = 6.1\ mm$$

The conclusion is that a 6-mm-diameter lead sphere launched at 5 mm/μsec will produce about the same impact stress history on an iron target as a 11.5-mm-diameter iron sphere launched at the same velocity. The masses of the two spheres will be

$$M_{Fe} = \left[\frac{4}{3}\pi \left(\frac{1.15}{2}\right)^3 cm^3\right] \left[(7.85)\ \frac{gm}{cm^3}\right] = 6.25\ gm$$

$$M_{Pb} = \left[\frac{4}{3}\pi \left(\frac{0.19}{2}\right)^3 cm^3\right] \left[(11.4)\ \frac{gm}{gm^3}\right] = 1.29\ gm$$

The sublimation energies given by Kohn[9] are:

$$E_s(F_e) = 7.36 \times 10^{10}\ ergs/gm$$

$$E_s(P_b) = 0.9155 \times 10^{10}\ ergs/gm$$

The internal energies produced by the shock wave are given approximately by

$$E \cong \frac{1}{2}\ \frac{P}{\rho_o}\left(1 - \frac{\rho_o}{\rho}\right)$$

The above information is summarized in the following table:

Table A-1

APPROXIMATE CONDITIONS FOR IDENTICAL IMPACT STRESS HISTORIES ON IRON TARGETS BY IRON AND LEAD SPHERES

Material	Impact Velocity (mm/μsec)	Impact Pressure (kbar)	Pressure Duration (μsec)	Projectile Diameter (mm)	Projectile Mass (gm)	Sublimation Energy (erg/gm)	Shock Energy (erg/gm)	Projectile Kinetic Energy (erg)
Iron	5	1500	1.7	11.5	6.3	7.4×10^{10} (1770 cal)	3×10^{10}	7.9×10^{10}
Lead	5	1500	1.7	6.0	1.3	0.92×10^{10} (220 cal)	3.8×10^{10}	1.6×10^{10}

The table shows that the lead projectile should receive enough shock energy to vaporize it upon pressure relief, whereas the iron projectile does not. Thus, a possible contribution to the impulse delivered to the target may arise from blow off of the lead projectile.

Note that the lead projectile requires only one-fifth the kinetic energy of the iron projectile to produce about the same impact stress history. In view of the possible gains from late-time blow off, lead would appear to be a promising hypervelocity projectile material.